ISSN 1674-1056
http://cpb.iphy.ac.cn
http://iopscience.iop.org/cpb
中国物理 B
Chinese Physics
中国物理
Chinese Physics B

Role of the spin anisotropy of the interchain interaction in weakly coupled antiferromagnetic Heisenberg chains

Yuchen Fan(樊宇辰), Rong Yu(俞榕)

Citation: Chin. Phys. B . 2020, 29(5): 057505 . **doi:** 10.1088/1674-1056/ab820b
Journal homepage: http://cpb.iphy.ac.cn; http://iopscience.iop.org/cpb

What follows is a list of articles you may be interested in

Exact solutions of an Ising spin chain with a spin-1 impurity

Xuchu Huang(黄旭初)
Chin. Phys. B . 2017, 26(3): 037501 . **doi:** 10.1088/1674-1056/26/3/037501

Interplay between spin frustration and magnetism in the exactly solved two-leg mixed spin ladder

Yan Qi(齐岩), Song-Wei Lv(吕松玮), An Du(杜安), Nai-sen Yu(于乃森)
Chin. Phys. B . 2016, 25(11): 117501 . **doi:** 10.1088/1674-1056/25/11/117501

Exact solution of Heisenberg model with site-dependent exchange couplings and Dzyloshinsky-Moriya interaction

Yang Li-Jun, Cao Jun-Peng, Yang Wen-Li
Chin. Phys. B . 2015, 24(10): 107502 . **doi:** 10.1088/1674-1056/24/10/107502

The spin dynamics of the random transverse Ising chain with a double-Gaussian disorder

Liu Zhong-Qiang, Jiang Su-Rong, Kong Xiang-Mu
Chin. Phys. B . 2014, 23(8): 087505 . **doi:** 10.1088/1674-1056/23/8/087505

Dynamics of one-dimensional random quantum *XY* system with Dzyaloshinskii–Moriya interaction

Li Yin-Fang, Kong Xiang-Mu
Chin. Phys. B . 2013, 22(3): 037502 . **doi:** 10.1088/1674-1056/22/3/037502

Role of the spin anisotropy of the interchain interaction in weakly coupled antiferromagnetic Heisenberg chains*

Yuchen Fan(樊宇辰) and Rong Yu(俞榕)†

Department of Physics and Beijing Key Laboratory of Opto-electronic Functional Materials and Micro-nano Devices, Renmin University of China, Beijing 100872, *China*

(Received 19 January 2020; revised manuscript received 16 March 2020; accepted manuscript online 23 March 2020)

In quasi-one-dimensional (q1D) quantum antiferromagnets, the complicated interplay of intrachain and interchain exchange couplings may give rise to rich phenomena. Motivated by recent progress on field-induced phase transitions in the q1D antiferromagnetic (AFM) compound $YbAlO_3$, we study the phase diagram of spin-1/2 Heisenberg chains with Ising anisotropic interchain couplings under a longitudinal magnetic field via large-scale quantum Monte Carlo simulations, and investigate the role of the spin anisotropy of the interchain coupling on the ground state of the system. We find that the Ising anisotropy of the interchain coupling can significantly enhance the longitudinal spin correlations and drive the system to an incommensurate AFM phase at intermediate magnetic fields, which is understood as a longitudinal spin density wave (LSDW). With increasing field, the ground state changes to a canted AFM order with transverse spin correlations. We further provide a global phase diagram showing how the competition between the LSDW and the canted AFM states is tuned by the Ising anisotropy of the interchain coupling.

Keywords: quasi-one-dimensional quantum antiferromagnets, Heisenberg spin chain, longitudinal spin density wave

PACS: 75.10.Pq, 75.50.Ee, 75.30.Fv, 75.30.Gw **DOI:** 10.1088/1674-1056/ab820b

1. Introduction

In contemporary condensed matter physics, many important concepts, ranging from the spin–charge separation[1] to the symmetry-protected topological order,[2] originate from one-dimensional (1D) systems. Studies on these systems keep active, and major progress has been made over the past decade in many quasi-one-dimensional (q1D) antiferromagnetic (AFM) systems.[3–12] The 1D AFM spin chain is also one of the best theoretically understood quantum many-body systems. For instance, the spin-1/2 XXZ chain, as a paradigmatic model, is well described by a Tomonaga–Luttinger liquid (TLL), which is a disordered state caused by strong quantum fluctuations. Under a longitudinal magnetic field, the spin correlation functions of the XXZ chain exhibit a power-law decay and can be expressed as

$$\begin{aligned} &\langle S_0^x S_r^x\rangle \simeq (-1)^r r^{-\eta}, \\ &\left\langle S_0^z S_r^z\right\rangle - \langle S^z\rangle^2 \simeq \cos\left(2k_{\mathrm{F}} r\right) r^{-\frac{1}{\eta}}, \end{aligned} \tag{1}$$

where k_{F} is defined as $k_{\mathrm{F}} = \pi\left(1/2 - \langle S^z\rangle\right)$ and refers to the Fermi wave number of the 1D spinless fermions mapped from the spin model by the Jordan–Wigner transformation.[1] η is the TLL exponent and varies with the applied magnetic field. It is easy to see that the value of η determines the dominant spin correlation. When the exchange coupling is Heisenberg or has an XY anisotropy, $\eta < 1$, and the transverse spin correlation always dominates. On the other hand, for an Ising anisotropic exchange coupling, there exists an η inversion at a crossover field h_{inv}. For $h < h_{\mathrm{inv}}$, $\eta > 1$, the longitudinal spin correlation dominates, and for $h > h_{\mathrm{inv}}$, $\eta < 1$, the dominant spin correlation changes to the transverse one, as in the case of a Heisenberg chain.[13]

The physics described above can be realized in many compounds. For example, $BaCo_2V_2O_8$ and $SrCo_2V_2O_8$ have shown to be ideal weakly-coupled spin-1/2 antiferromagnetic XXZ chains with an Ising anisotropy. In certain field regime, the neutron diffraction measurements discovered an incommensurate AFM state,[13–16] which is understood as a longitudinal spin density wave (LSDW).[17–19] In this LSDW state, the dominant spin correlation is longitudinal, and takes the form of Eq. (1) along the chain direction. Both η and k_{F} are tuned by the applied magnetic field, and this causes the modulation of the ordering wave vector

$$|\Delta Q| = 1 - 2k_{\mathrm{F}} = 2m^z, \tag{2}$$

where $m^z = \langle S^z\rangle$ is the uniform magnetization. Such a modulated ordering wave vector is a characteristic of the underlying 1D physics. Further increasing the magnetic field, the dominant spin correlation changes to be transverse. As a consequence, the ground state turns to be a canted AFM state,

*Project supported by the National Natural Science Foundation of China (Grant No. 11674392), the Ministry of Science and Technology of China, National Program on Key Research Project (Grant No. 2016YFA0300504), and the Research Funds of Remnin University of China (Grant No. 18XNLG24). R.Y. acknowledges the hospitality at Tsung-Dao Lee Institute.

†Corresponding author. E-mail: rong.yu@ruc.edu.cn

© 2020 Chinese Physical Society and IOP Publishing Ltd

which is usually denoted as the TAF order.[16,20]

These findings lead to the naive thought that the essential physics in q1D antiferromagnets is dictated by the intrachain exchange coupling because the interchain coupling is too weak, compared to the intrachain one, to affect the dominant spin correlation. However, there exist rare cases that the interchain coupling, though weak, is relevant to the low-energy physics of the system. For example, the frustrated interchain couplings may give rise to exotic ground states in a spin model for $CoNb_2O_6$.[21]

A recent surprise is in the q1D antiferromagnet $YbAlO_3$. On the one hand, the intrachain exchange coupling of this compound is found to be almost isotropic in the spin space (namely, Heisenberg-like), on the other hand, an incommensurate AFM state induced by the magnetic field is observed.[22] In the incommensurate AFM state, it is found that the modulation of the ordering wave vector follows Eq. (2), which strongly implies that the AFM order is an LSDW. A major puzzle is then how the LSDW order would arise from the coupled Heisenberg chains. It has been suggested that the interchain coupling plays an important role,[22,23] and a recent work by the authors[24] unambiguously shows that an Ising spin anisotropy of the interchain coupling can enhance the longitudinal spin correlations of the coupled Heisenberg chains and stabilize the LSDW order. Nonetheless, a systematic study on how the global phase diagram is affected by the interchain Ising anisotropy is still lacking.

In this paper, we perform a thorough study on the effects of the interchain coupling in weakly coupled Heisenberg chains by using quantum Monte Carlo (QMC) simulations. Our results indicate that the Ising anisotropy in the interchain coupling, whenever the coupling is ferromagnetic (FM) or AFM, can enhance the longitudinal spin correlation and stabilize the incommensurate LSDW order. We further provide a global phase diagram to show how the LSDW and the TAF states compete as the interchain Ising anisotropy increases. These results not only solve the puzzle on the origin of the incommensurate AFM order observed in $YbAlO_3$, but also highlight the crucial role of the interchain couplings in q1D antiferromagnets, which was certainly overlooked in previous studies.

2. Model and method

We consider an effective spin-1/2 model for $YbAlO_3$, which includes weakly coupled Heisenberg spin chains defined on a cubic lattice. The Hamiltonian reads

$$\mathcal{H} = J_c \sum_i \boldsymbol{S}_i \cdot \boldsymbol{S}_{i+c} - g\mu_B H \sum_i S_i^z + J_{ab} \sum_{i,\delta=\{a,b\}} \left[\varepsilon \left(S_i^x S_{i+\delta}^x + S_i^y S_{i+\delta}^y \right) + S_i^z S_{i+\delta}^z \right]. \quad (3)$$

Here $\boldsymbol{S}_i = \{S_i^x, S_i^y, S_i^z\}$ is a spin-1/2 operator defined at site i. J_c and J_{ab} are respectively the intrachain and interchain exchange couplings between the nearest neighboring spins. H is the applied longitudinal magnetic field. Note that generically the longitudinal direction z-axis is different from the chain direction c-axis, and this is also the case for $YbAlO_3$.[22] ε denotes the spin anisotropy of the interchain coupling. In this work, we focus on the effect of the Ising anisotropy of the interchain coupling by setting $\varepsilon < 1$ and keeping the intrachain interaction to be Heisenberg (isotropic in the spin space) antiferromagnetic.

For simplicity, we set the gyromagnetic factor g and the Bohr magneton μ_B to be 1, and set $J_c = 1$ to be the energy unit. In the discussion below, we will use the dimensionless reduced field and reduced temperature, which are defined as $h = g\mu_B H/J_c$ and $t = k_B T/J_c$, respectively. The interchain interactions in $YbAlO_3$ are rather complicated, contain both FM and AFM couplings.[22,25] Since the ordering wave vector in the incommensurate AFM state is at $(0,0,Q)$, we simplify the interchain couplings in the model by assuming them to be all FM ($J_{ab} < 0$). In the following, we take $\varepsilon = 0.25$ and $J_{ab} = -0.2J_c$ for demonstration. The effects of varying these parameters and the connection to experiments are discussed in Subsections 3.2 and 3.3, respectively. We examine the field induced phase diagram of the model by performing numerically exact QMC simulations based on the stochastic series expansion (SSE) algorithm.[26,27] In the simulations, the largest system size is $20 \times 20 \times 128$ and the lowest temperature accessed is $t = 0.01$.

3. Results and discussion

3.1. Phase diagram and the field induced LSDW order

We have calculated the magnetization of the model defined in Eq. (3) with the applied field by taking $J_{ab} = -0.2$ and $\varepsilon = 0.25$. The result at $t = 0.05$ is shown in Fig. 1(a). The magnetization curve suggests a finite gap in the system for $h \lesssim 0.5$, and the magnetization gets saturated for $h \gtrsim 1.75$. In between, it changes its curvature at $h \sim 0.8$. These features imply that at low temperatures the system experiences a number of phase transitions tuned by the field. We then study the field induced phase diagram, which is shown in Fig. 1(b) from our calculation. The thermal phase transition at each field value is determined by the peak temperature of the specific heat data, which are illustrated in Fig. 2. To understand the nature of the low-temperature phases, we examine the normalized longitudinal and transverse spin structure factors in these phases

$$\mathcal{S}^{zz}(\boldsymbol{q}) = \frac{1}{N^2} \sum_{ij} e^{i\boldsymbol{q}\cdot(\boldsymbol{r}_i - \boldsymbol{r}_j)} \left\langle S_i^z S_j^z \right\rangle, \quad (4)$$

$$\mathcal{S}^{xy}(\boldsymbol{q}) = \frac{1}{2N^2} \sum_{ij} e^{i\boldsymbol{q}\cdot(\boldsymbol{r}_i - \boldsymbol{r}_j)} \left\langle S_i^x S_j^x + S_i^y S_j^y \right\rangle. \quad (5)$$

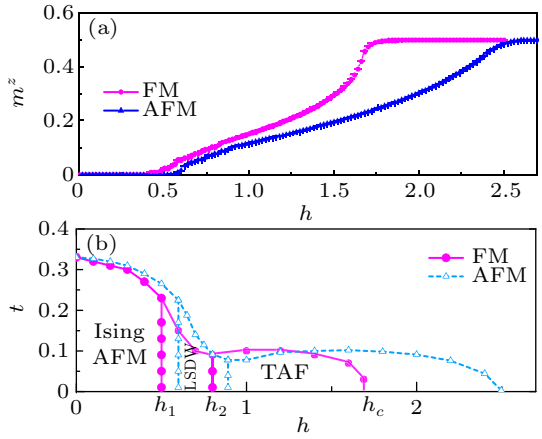


Fig. 1. (a) Field dependence of the magnetization of the model in Eq. (3) with an FM interchain coupling (magenta line) $J_{ab} = -0.2$, $\varepsilon = 0.25$, compared to that with an AFM interchain coupling (blue line) $J_{ab} = 0.2, \varepsilon = 0.25$. Both curves are obtained at $t = 0.05$ with the system size $20 \times 20 \times 128$. (b) The phase diagram in the h–t plane with FM (magenta) and AFM (blue, adapted from Ref. [24]) interchain couplings, $|J_{ab}| = 0.2$, $\varepsilon = 0.25$.

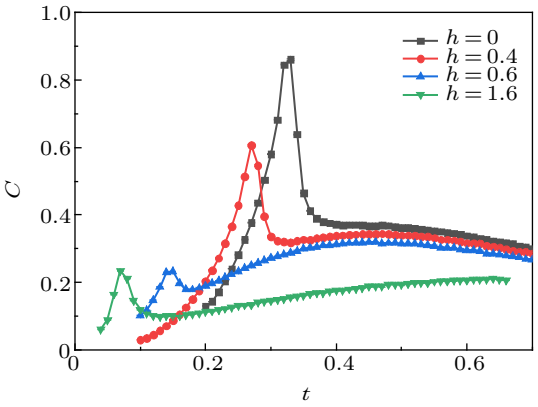


Fig. 2. Temperature dependence of the specific heat C at various fields for the model with $J_{ab} = -0.2$, $\varepsilon = 0.25$. The system size is $24 \times 24 \times 24$. The peak in C indicates a thermal transition to the magnetically ordered phase, which is used to determine the phase boundary in Fig. 1(b).

As shown in Fig. 3(a), for $h < h_1 \approx 0.5$, the longitudinal structure factor $\mathcal{S}^{zz}(\boldsymbol{q})$ has a single sharp peak at wave vector $\boldsymbol{q} = (0, 0, \pi)$, signaling an Ising AFM (Néel) order. Increasing the field, this peak splits into two, respectively located at incommensurate $\boldsymbol{q} = (0, 0, \pi \pm \Delta Q)$, as shown in Fig. 3(b). The modulated wave vector ΔQ varies with the magnetic field and follows the relation in Eq. (2), as shown in Fig. 3(d). This indicates that the incommensurate AFM state is an LSDW. Further increasing the field for $h > h_2 \approx 0.82$, the peak in $\mathcal{S}^{zz}$ vanishes, while a peak in the transverse structure factor $\mathcal{S}^{xy}(\boldsymbol{q})$ arises at the wave vector $\boldsymbol{q} = (0, 0, \pi)$. The ground state of the system then changes from the LSDW to the canted TAF state. This canted TAF order persists up to a quantum critical point (QCP) at $h_c \sim 1.7$, above which the spins are eventually polarized by the magnetic field. The polarization of the spins leads to a saturation of the magnetization at $h > h_c$. As shown in Fig. 1(a), the magnetization is very closed to the saturated value $m^z = 1/2$ for $h \gtrsim 1.75$ at $t = 0.05$. This justifies that the simulated system already approaches to its ground state at this temperature. The entire phase diagram is clearly presented in Fig. 1(b).

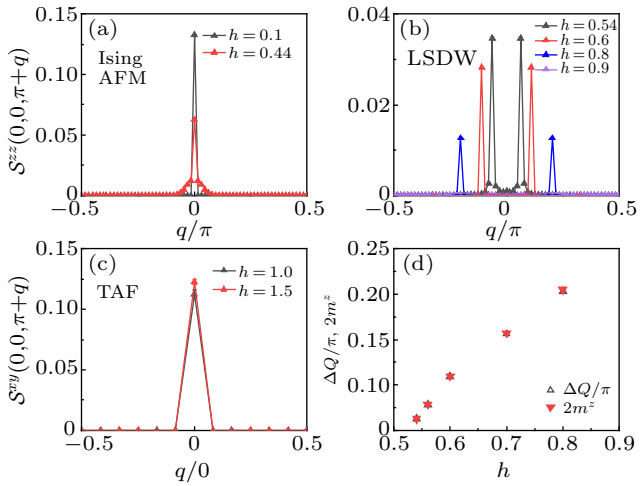


Fig. 3. Longitudinal spin structure factor $\mathcal{S}^{zz}(0, 0, \pi + q)$ in (a) the Ising AFM (Néel) phase and (b) the LSDW phase. The system size is $20 \times 20 \times 128$. (c) Transverse spin structure factor $\mathcal{S}^{xy}(0, 0, \pi + q)$ in the TAF phase. The system size is $24 \times 24 \times 24$. (d) Field dependence of the modulated ordering wave vector ΔQ and the magnetization, satisfying the relation in Eq. (2). The model parameters used are $J_{ab} = -0.2$ and $\varepsilon = 0.25$, with simulations performed at $t = 0.05$.

From the results above, one clearly sees that the LSDW order can be stabilized by the FM interchain coupling. In Fig. 1, we have also compared our results to those with the AFM interchain coupling.[24] It is interesting to see that either the FM or the AFM interchain coupling can stabilize the LSDW phase. This can be understood as follows: the LSDW state is characterized by incommensurate AFM spin correlations along the chain direction. The spin correlations perpendicular to the chain directions can be either FM or AFM. Once the exchange couplings are unfrustrated, either the interchain or the intrachain coupling can enhance the AFM spin correlation along the chain direction. Our results also show that the saturation field h_c depends strongly on the sign of the interchain coupling. This is easily understood because the spins along two adjacent chains are much easier to be polarized by the field when they are coupled by the FM interaction.

3.2. The effect of Ising anisotropy of the interchain coupling

In previous studies,[18,19] the stabilization of the LSDW order requires an Ising anisotropy in the intrachain exchange coupling. For coupled Heisenberg chains, the interchain coupling was treated as an internal field within the mean-field approximation.[18] Because the interchain spin fluctuations were completely ignored in the mean-field approach, the dominant spin correlations in the coupled Heisenberg chains would still be transverse. Therefore, an LSDW order could not appear even if the interchain coupling was strongly Ising

anisotropic. Our numerical method, on the other hand, takes full effects of spin fluctuations of the interchain coupling, and reveals a different way to settle down the LSDW phase: The Ising anisotropy in the interchain coupling can significantly enhance the longitudinal spin correlations and stabilize the LSDW state at low temperatures.

To see this more clearly, we study the phase diagram of the model in Eq. (3) by fixing $J_{ab} = -0.2$ and varying the Ising anisotropy factor ε. As shown in Fig. 4(a), when taking $\varepsilon = 0.5$, i.e., a smaller Ising anisotropy, there is a direct first-order transition between the Ising AFM (Néel) and the TAF phases, and the LSDW state cannot be stabilized in the field induced phase diagram.

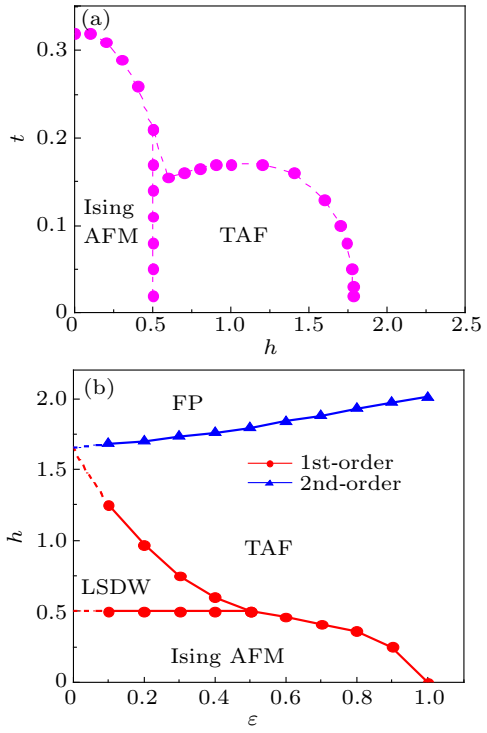


Fig. 4. (a) Phase diagram in the t–h plane for $J_{ab} = -0.2$, $\varepsilon = 0.5$. (b) Ground-state phase diagram in the ε–h plane for $J_{ab} = -0.2$. FP refers to fully polarized. The QMC simulations are performed at $t = 0.02$ (corresponds to $T \sim 50$ mK for $YbAlO_3$) with system size $20 \times 20 \times 128$ to ensure the convergence to the ground state. The error bar of the phase boundary data is about 0.02, which is smaller than the symbol size. The extrapolations are shown as the dashed lines.

To see how the Ising anisotropy affects the phase diagram quantitatively, we determine the ground-state phase diagram in the ε–h plane in Fig. 4(b). In the isotropic limit ($\varepsilon = 1$), the TAF order is stabilized above an infinitesimal field until the spins are fully polarized. This implies that the dominant spin correlation is transverse, which is consistent with the previous results of a Heisenberg chain.[13] With increasing the Ising anisotropy of the interchain coupling (decreasing ε), the dominant spin correlation changes to be longitudinal at low fields, but keeps to be commensurate. This stabilizes the Ising AFM (Néel) order at low fields. For $\varepsilon \lesssim 0.49$, the incommensurate longitudinal spin correlation dominates in certain field regimes, and as a consequence, the LSDW order appears to be the ground state. As shown in Fig. 4(b), the phase boundary between the TAF and LSDW phases depends strongly on ε, suggesting strong competition between these two phases with varying the Ising anisotropy. In the complete Ising limit, namely, $\varepsilon \to 0$, the transverse spin correlation is limited to be within each chain, and a global TAF order cannot be stabilized. The phase boundaries among the Ising AFM, LSDW, and TAF phases are all first-order, while there is a second-order quantum phase transition (QPT) between the TAF and the fully polarized (FP) phase at h_c, where the magnetization saturates at zero temperature. It would be interesting to study the QPT directly from the LSDW to the FP phase at $\varepsilon = 0$. But unfortunately, our QMC simulation becomes very inefficient and cannot provide any reliable results in this limit. We defer such a study to a future work with more advanced theoretical approach.

3.3. Implication for $YbAlO_3$

We now discuss the implication of our results for $YbAlO_3$. The intrachain exchange coupling of $YbAlO_3$ is found to be almost isotropic, but the interchain coupling, mediated by the dipole–dipole interaction, contains strong Ising anisotropy.[22,25] These key features are fully described by our model in Eq. (3) with $\varepsilon < 1$. In the calculations, we take the estimated values $J_c \sim 0.21$ meV, $g \sim 7.6$, and $|J_{ab}|/J_c \sim 0.2$ for $YbAlO_3$ from experiments.[22] There is no estimated value for ε. But as shown in Fig. 4(b), we find that the LSDW state can be stabilized over a broad ε regime in the ground-state phase diagram. This LSDW state provides a natural explanation to the observed incommensurate AFM state in $YbAlO_3$.[22] Here the stabilization of the LSDW state is from the Ising anisotropy of the interchain coupling, which is beyond the interchain mean-field scenario in previous studies.[18] Without fine tuning we simply take $\varepsilon = 0.25$ and perform the simulations. The resulting phase diagram qualitatively agrees with the experimental one in Ref. [22]. For example, the LSDW order shows up at $h_1 \sim 0.5$, and the magnetization saturates at $h_c \sim 1.75$. These two field values correspond to about 0.3 T and 0.9 T, respectively, and they are close to the experimental values of 0.35 T and 1.1 T. Note that a simplification of our model is that we assume the interchain coupling to be all FM. But in $YbAlO_3$, the real interchain interactions contain both FM and AFM couplings. We also perform the simulation with AFM interchain coupling,[24] and indeed find that the LSDW state is stabilized within approximately similar field range, as shown in Fig. 1(b). This result indicates that our model captures the essential physics in $YbAlO_3$. The spin frustration by including both FM and AFM interchain couplings likely acts as a secondary effect which fine tunes the phase boundaries.

4. Conclusion

We study the phase diagram of an effective spin-1/2 model of Heisenberg chains coupled by Ising anisotropic interchain interactions. We find that the Ising anisotropy of the interchain coupling can enhance the incommensurate longitudinal AFM correlation and stabilize an LSDW phase. We show that the LSDW phase appears robustly with either FM or AFM interchain coupling when the Ising anisotropy is sufficiently strong. These findings explain the recently observed incommensurate AFM state in coupled Heisenberg chain compound $YbAlO_3$. Compared to previous theories, our results reveal a different way in stabilizing the LSDW order in q1D antiferromagnets, and underscore the key role of the interchain interaction in these materials.

References

[1] Giamarchi T 2004 *Quantum Physics in One Dimension* (Oxford: Oxford Univ. Press)

[2] Gu Z C and Wen X G 2009 *Phys. Rev. B* **80** 155131

[3] Coldea R, Tennant D A, Wheeler E M, Wawrzynska E, Prabhakaran D, Telling M, Habicht K, Smeibidl P and Kiefer K 2010 *Science* **327** 177

[4] Wu J, Kormos M and Si Q 2014 *Phys. Rev. Lett.* **113** 247201

[5] Wang Z, Wu J, Yang W, *et al.* 2018 *Nature* **554** 219

[6] Wang Z, Schmidt M, Loidl A, *el al.* 2019 *Phys. Rev. Lett.* **123** 067202

[7] Bera A K, Wu J, Yang W, Wang Z, Bewley R, Boehm M, Bartkowiak M, Prokhnenko O, Klemke B, A T M Nazmul Islam, Law J M and Lake B 2019 arXiv:1909.00146 [cond-mat.str-el]

[8] Faure Q, Takayoshi S, Petit S, *et al.* 2018 *Nat. Phys.* **14** 716

[9] Cui Y, Zou H, Xi N, *et al.* 2019 *Phys. Rev. Lett.* **123** 067203

[10] Zapf V, Jaime M and Batista C D 2014 *Rev. Mod. Phys.* **86** 563

[11] Yu R, Yin L, Sullivan N S, *et al.* 2012 *Nature* **489** 379

[12] Faizi E and Eftekhari H 2015 *Chin. Phys. Lett.* **32** 100303

[13] Kimura S, Takeuchi T, Okunishi K, Hagiwara M, He Z, Kindo K, Taniyama T and Itoh M 2008 *Phys. Rev. Lett.* **100** 057202

[14] Kimura S, Matsuda M, Masuda T, Hondo S, Kaneko K, Metoki N, Hagiwara M, Takeuchi T, Okunishi K, He Z, Kindo K, Taniyama T and Itoh M 2008 *Phys. Rev. Lett.* **101** 207201

[15] Klanjsek M, Horvatic M, Kramer S, Mukhopadhyay S, Mayaffre H, Berthier C, Canevet E, Grenier B, Lejay P and Orignac E 2015 *Phys. Rev. B* **92** 060408(R)

[16] Shen L, Zaharko O, Birk J O, Jellyman E, He Z and Blackburn E 2019 *New J. Phys.* **21** 073014

[17] Haldane F D M 1980 *Phys. Rev. Lett.* **45** 1358

[18] Okunishi K and Suzuki T 2007 *Phys. Rev. B* **76** 224411

[19] Suzuki T, Kawashima N and Okunishi K 2007 *J. Phys. Soc. Jpn.* **76** 123707

[20] Grenier B, Simonet V, Canals B, Lejay P, Klanjšek M, Horvatić M and Berthier C 2015 *Phys. Rev. B* **92** 134416

[21] Lee S, Kaul R K and L Balents 2010 *Nat. Phys.* **6** 702

[22] Wu L S, Nikitin S E, Wang Z, *et al.* 2019 *Nat. Commun.* **10** 698

[23] Agrapidis C E, J van den Brink and Nishimoto S 2019 *Phys. Rev. B* **99** 224423

[24] Fan Y C, Yang J H, Yu W Q, Wu J D and Yu R 2020 *Phys. Rev. Research* **2** 013345

[25] Wu L S, Nikitin S E, Brando M, *et al.* 2019 *Phys. Rev. B* **99** 195117

[26] Syljuåsen O F and Sandvik A W 2002 *Phys. Rev. E* **66** 046701

[27] Alet F, Wessel S and Troyer M 2005 *Phys. Rev. E* **71** 036706